Proceedings of the Sixth International Conference on
Railway Technology: Research, Development and Maintenance
Edited by: J. Pombo
Civil-Comp Conferences, Volume 7, Paper 7.1
Civil-Comp Press, Edinburgh, United Kingdom, 2024
ISSN: 2753-3239, doi: 10.4203/ccc.7.7.1

Fatigue Crack Damage Detection Using Gaussian Mixture Model Based on Information Entropy Under Time-Varying Temperature

X. Zhang, T. Wang and J. Yang
School of Traffic & Transportation Engineering,
Central South University, Changsha, China

Abstract

High-speed train structures operate under time-varying conditions, which poses a significant challenge in the field of PHM due to uncertainties introduced in the extraction of damage indexes from signals. This paper presents a new fatigue crack size quantification method based on information entropy unde variable temperature environment. Two new information entropy are proposed: energy singular spectral entropy (ES) and power singular spectral entropy (PS). The baseline Gaussian mixture model is constructed on the information entropy acquired under time-varying temperature when the structure is in a healthy state. The on-line Gaussian mixture model is constructed through the online update mechanism of moving feature sample set. The minimum matching Kullback–Leibler (KL) distance of the probability component is used to quantitatively characterize the cumulative migration trend of the Gaussian mixture model under damage to realize damage detection. The framework proposed in this paper is applied to Lamb wave data collected from fatigue crack experiments under variable temperature environment. The experimental results verify the reliable fatigue crack detection performance of Gaussian mixture model-KL method under variable temperature environment.

Keywords: Lamb wave, information entropy, fatigue crack, time-varying temperature, Gaussian mixture model, high speed train.

1 Introduction

Structural health monitoring (SHM) is a crucial technology used to tackle safety and maintenance issues of high speed trains.[1]. Plate- and pipe-like aluminum alloy structures have been widely used in high speed trains, according to the advantage of light weight, high strength and corrosion resistance[2]. Due to the dynamic loading, material defects, improper installation and severe service environment exposure, the aluminum alloy structures naturally tend to fatigue cracks growth[3]. The fatigue damage will harm the structural integrity and even cause fateful consequence. Therefore, it is of great significance to study the damage monitoring technology under time-varying environment for improving the operation stability of high-speed trains.

Lamb waves (LW) have shown great potential in SHM of high-speed trains. A large number of studies have used LW for damage identification. The traditional LW detection method extracts the damage indexes, and uses the damage index to quantitatively characterize the crack length [4][5]. Chen proposed a nonlinear Lamb wave detection system[6]. Yuan et al. used the piezoelectric transducers (PZTs)-based active Lamb wave method to conduct online crack monitoring. They proposed deterministic resampling particle filter for fatigue crack growth prediction, which can overcome the sample impoverishment problem[7]. Wang et al. presented the method of physical and virtual time reversing of nonlinear Lamb waves for fatigue crack detection and quantification[8]. Lu et al. proposed a Lamb wave matching pursuit algorithm to overcome fatigue crack quantification[9]. As a consequence, the diverse Lamb wave inspection approaches show great potential for fatigue crack detection.

The effectiveness of Lamb wave for fatigue crack monitoring has been demonstrated in previous studies. However, due to the complexity of wave propagation across cracks, few investigations have focused on the impact of temperature. Temperature is one of the main environmental factors that can affect the practical application of Lamb wave-based structural health monitoring (SHM), as it can alter the wave velocities and amplitudes. Moreover, ambient temperature can interfere with the detection of real damage information and reduce the reliability of the results. Therefore, it is crucial to address the effect of temperature on guided waves to enhance the practical applicability of Lamb wave-based SHM. It needs to be combined with other mathematical analysis methods to achieve the purpose of better extraction of damage indexes. Information entropy can be combined with a variety of signal decomposition algorithms and mathematical analysis methods[9-11]. Therefore, many scholars establish information entropy based on time domain and frequency domain analysis methods to characterize the fault characteristics of signals. Information entropy is a combination of entropy and information theory and is defined as a measure of the uncertainty of an event[10]. It can be used as a signal feature to describe the amount of information transmitted by the signal. Ma Hassan[11] and others adopted the feature extraction method of wavelet decomposition and a combination of Shannon entropy and the cross bispectrum, resulting in the extracted features retaining more complete fault information. Shi Guoliang[12] used permutation and combination entropy as feature vectors for fault classification and

fault identification. Damage indexes based on information entropy can often contain more kinds of information and better characterize fault information. Therefore, different information entropies will be established in this paper to achieve effective damage indexes for Lamb wave signals under time-varying temperature. Probability and statistics techniques have been applied to mitigate the impact of temperature on LW-based SHM. For instance, the Gaussian mixture model (GMM) has shown great potential in detecting damage under environmental variations [13][14]. Wang et al. established Gaussian mixture models to reconstruct various fault signals in the phase space, and then used these models to classify bearing faults[15]. QIMA et al. proposed a new method based on Dirichlet process Gaussian mixture model (DP-GMM), and developed a new feature vector for structural health monitoring in time-varying environment[16].

Due to the complexity of Lamb waves, dispersion and multimodal effects and time-varying temperature, there are many uncertain problems. Therefore, it is necessary to adopt the damage index with high robustness and more information to improve the precision of GMM. GMM with high accuracy, multiple indicators and strong robustness is expected to solve the problem of variable temperature crack monitoring. Inspired by this, a damage detection method based on GMM using information entropy is developed in this paper towards accurate detection of fatigue crack growth over a wide range of temperature variation. In this method, two new information entropy ES and PS are proposed based on EEMD and SSA algorithm. The GMM using information entropy under the influence of time-varying temperature is established. To enable online tracking of damage progress, the proposed method incorporates an update mechanism that utilizes the mobile feature set and internal probability of the GMM. The updated probability can then be used to continuously monitor the damage progression in real-time. The effectiveness and precision of the method are demonstrated through a fatigue crack monitoring test that involves time-varying temperature.

The structure of this paper is as follows. the information entropy measures ES and PS is presented in Section 2. the in-depth introduction to the GMM and KL is provided in Section 3. The fatigue crack detection test conducted under time-varying temperature is discussed in Section 4. the conclusions drawn from this study in Section 5.

2 Information entropy of Lamb wave

The calculation process of the two new information entropy is mainly divided into two parts Ensemble Empirical Mode Decomposition (EEMD) [17]and Singular Spectrum Analysis (SSA) [18]. The algorithm can adaptively decompose the complex signal into several Intrinsic Mode Functions (IMF) [19][20], and the decomposed IMF components can reflect the local characteristic information of the original signal at different time scales. The mean value of IMF component obtained after decomposition is selected as the decomposed signal. The mean value of IMF component can eliminate the additional noise effect and retain the useful signal mapped to the corresponding characteristic scale. Then these signals are analyzed by SSA, and the reconstructed signal sequence is obtained. The energy singular spectral

entropy (ES) and the power singular spectral entropy (PS) can be calculated by replacing the original signal with a reconstructed time series. The EEMD and SSA algorithm flow chart is shown in Figure1.

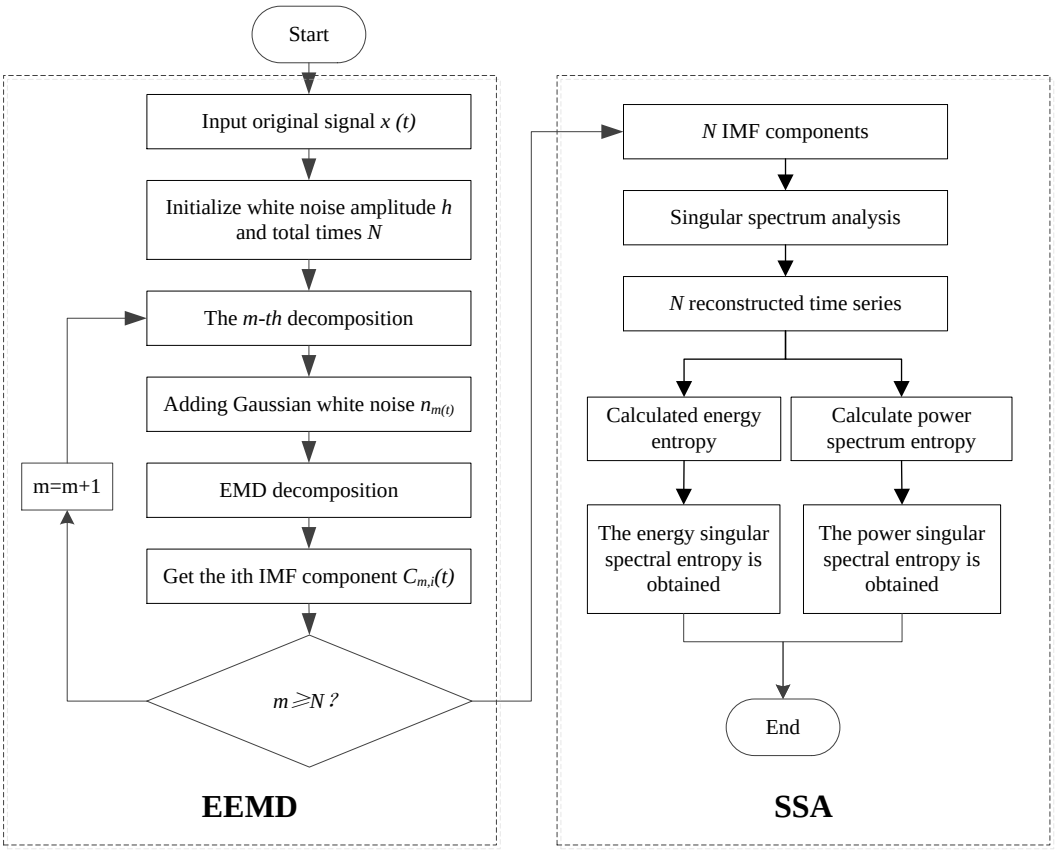

Figure 1: Flow Chart of EEMD and SSA Algorithm.

The information entropy extraction process of non-stationary signal in time-varying temperature environment is as follows: Each signal data collected from the PZT is continuous time series $x(t)$, which is decomposed by EEMD. n $IMF(t)$ components $IMF_1(t)$, $IMF_2(t)$,..., $IMF_n(t)$ are obtained by EEMD analysis of $x(t)$. The reconstructed signal $y_i(t), i=1,2,3\ldots,N$ is obtained by SSA analysis of n $IMF(t)$ components. The specific calculation process of EEMD and SSA algorithm is as follows: Gaussian white noise $n(t)$ is added to the original signal $x(t)$ many times. The m-th Gaussian white noise signal is added as:

$$x(t) = x(t) + h \times n_m(t) \quad (\mathrm{m} \le \mathrm{N}) \tag{1}$$

where $n_m(t)$ is the white noise added in the m-th time, h is the amplitude coefficient of the noise, and N is the number of EMD decomposition aggregations, generally taken as 100.

EEMD decomposition is performed on the signal $x_m(t)$ with white noise added to obtain n IMF components $c_{m,i}(t)$, $i \le n$ and a residual component $r_{m,n}(t)$. When m <

n, repeat the above steps and add different white noise signals each time. Then the average value $\overline{c_i}$:

$$\overline{c_i} = \frac{\sum_{m=1}^{N} c_{m,i}}{N} \tag{2}$$

$\overline{c_i}$ is the final eigenmode function. SSA is performed on the IMF components, and an appropriate window length $m(2 \leqslant m \leqslant t)$ is selected. The one-dimensional signal sequence $IMF_i(t)$ is transformed into a multidimensional sequence to obtain the trajectory matrix X:

$$X = (x_{ij})_{i,j=1}^{n,m} = \begin{pmatrix} x_1 & x_2 & \cdots & x_m \\ \vdots & \vdots & \vdots & \vdots \\ x_n & x_{n+1} & \cdots & x_t \end{pmatrix} \tag{3}$$

The singular value of matrix X is calculated, and it is decomposed to obtain m indexes and their corresponding eigenvectors:

$$Y(t) = \sum_{j=1}^{m} \frac{X}{\alpha_p}, i = p - j + 1, 0 < i < n+1 \tag{4}$$

where when $p < m$, $\alpha_p = p$. When $p > t - m + 1$, $\alpha_p = t - p + 1$. When $m \le p \le t - m + 1$, $\alpha_p = m$.

Through the above calculation, the *IMF* component is reconstituted into a new time series, which can replace the *IMF* component as the input for calculating the traditional information entropy and obtaining two new information entropies PS and ES.

Energy singular spectral entropy

Energy singular spectral entropy can represent the complexity of signal energy. The information of different frequency bands in the signal is contained in different IMF components. The input of the algorithm is the IMF component of the new time series and the output is ES. The steps are as follows:

Calculate the energy of each reconstructed IMF component separately:

$$E_i = \int_{-\infty}^{\infty} IMF_i^2(t)dt, \quad i = 1, 2, \ldots, N \tag{5}$$

Calculate the proportion of the energy of each reconstructed IMF component to the total energy:

$$p_i = \mathrm{E}_i / \mathrm{E} \tag{6}$$

Calculate the ES of the signal $x(t)$ according to ^{p} [21]:

$$\mathrm{ES} = -\sum_{i=1}^{N} p_i \lg p_i \tag{7}$$

Power singular spectral entropy

According to the calculation principle of ES[22], the IMF component is also time reconstructed, and the new time series is used to calculate the PS instead of the IMF component. The input of the algorithm is the IMF component of the new time series and the output is PS. The steps are as follows:

Estimate the power spectrum of the reconstructed $IMF_i(t)$ according to the formula of the maximum entropy method, and obtain the corresponding power singular spectrum:

$$IMF_l(f) \approx \frac{a_0}{\left|1+\sum_{m=1}^{M} a_m e^{-j2\pi mfT}\right|^2} \tag{8}$$

where a_0 and a_m are the solutions of the Yule-Walker[22] equation $R_{xx}(x) = -\sum_{m=0}^{M} a_m R_{xx}(x-k), x > 0$.

Calculate the PS of signal[23]:

$$\mathrm{PS} = -\sum_{i=1}^{N} \alpha_i \log_{10} \alpha_i \tag{9}$$

where α_i is the proportion of the power spectrum value of the *i-th* reconstructed IMF component in the total PS.

Since the high-speed train is in service under the time-varying temperature environment, the damage indexes reflected by the signal in the time-frequency domain are not singular or regular. The ES and PS proposed in this paper decompose the original signal by EEMD and SSA, and transform the original signal of nonlinear and non-stationary signal into a new signal sequence with different characteristic scales. The information entropy eigenvalues es and PS proposed in this paper calculate the whole segment of signal and retain more complete fault information. Therefore, the ES and PS extracted in this paper can more clearly describe the fault information.

3. GMM Using Information Entropy

The principle of GMM damage detection based on information entropy is as follows. Information entropy is used to establish online GMM in the process of online detection. Under the influence of time-varying temperature, the probability distribution of the information entropy changes randomly. When crack damage occurs in the structure, the probability distribution of the Lamb information entropy of the structure exhibits cumulative migration different from that from the influence of time-varying temperature factors. Therefore, the structural damage state can be evaluated by the probability distribution migration trend of the online GMM relative to the baseline GMM. The probability distribution migration trend of the online GMM

relative to the baseline GMM can be used to evaluate the structural damage state in the proposed method. The damage detection framework is shown in Figure 2.

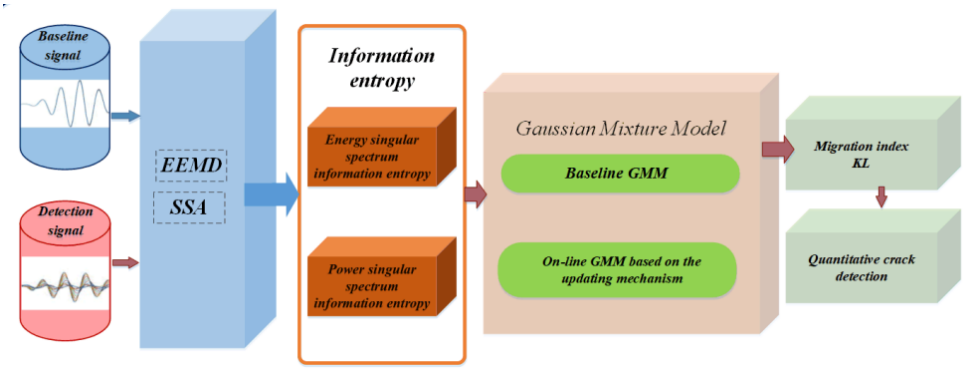

Figure 2: Damage detection framework based on GMM.

3.1 GMM principle and damage detection principle

According to the two kinds of information entropy obtained in the section 2, the damage index matrix S is constructed, which is defined as:

$$S=\begin{bmatrix} ES_1 & PS_1 \\ ES_2 & PS_2 \\ ES_3 & PS_3 \\ \vdots & \vdots \\ ES_K & PS_K \end{bmatrix}=\begin{bmatrix} S_1 \\ S_2 \\ S_3 \\ \vdots \\ S_K \end{bmatrix} \tag{10}$$

Suppose there are K LW signals in total. In the sample matrix, each row corresponds to a Lamb signal's damage indexes (ES, PS), and each column represents different signal values of a damage index.

The GMM equation is given by equation (11):

$$\Phi\left(S_K|\ \boldsymbol{\mu},\boldsymbol{\Sigma}\right)=\sum_{i=1}^{C} w_i\Phi_i\left(S_K|\ \boldsymbol{\mu}_i,\boldsymbol{\Sigma}_i\right) \tag{11}$$

C represents the quantity of gas components. $\boldsymbol{\mu}_i,\boldsymbol{\Sigma}_i$ and w_i are the mean, covariance matrix and mixing weight of Gaussian components respectively, i=1, 2, …C. The probability density is expressed as (12).

$$\Phi_i\left(S_K|\ \mu_i,\Sigma_i\right)=\frac{1}{(2\pi)^{d/2}\left|\Sigma_i\right|^{1/2}}\exp\left\{-\frac{1}{2}\left(S_K-\mu_i\right)^T\sum_i^{-1}\left(S_K-\mu_i\right)\right\} \tag{12}$$

The two main parameters that determine the GMM are the variance $\boldsymbol{\Sigma}_i$ and mean $\boldsymbol{\mu}_i$. To fit and update these parameters, K-means and EM algorithms are commonly used [24][25]. The EM algorithm is an expectation-maximization algorithm that estimates the missing parameters (i.e., hidden variables) in GMM, which can have multiple hidden variables [26].

While the EM algorithm can be used to build a GMM, it needs to be updated with new feature vectors in online damage monitoring. However, replacing a set of characteristics with a single feature vector results in a slower GMM update speed due to its low contribution. To address this, an update mechanism based on motion feature set and internal probability structure has been proposed [27][28]. Proposed an update mechanism based on motion feature set and internal probability structure. By adjusting or even changing the GMM probability structure, the new feature vector can be tracked quickly and stably.

In the process of online damage monitoring, to obtain a new feature vector, need to update the feature sample set $S=\{S_1, S_2,\ldots, S_K\}$. The update index is expressed as n. The feature sample set S is updated through the mobile update mechanism, that is, each time a new feature vector S_{K+1} is added as the last (latest) sample S, S_1 is removed from the first (oldest) sample S. The number of updated eigenvectors remains unchanged.

3.2 GMM Migration Index

After establishing the baseline GMM and the online GMM, the offset change of the latter relative to the former is quantified using the KL [29]. For a ϕ_i^0 in the baseline GMM ϕ^0, the KL distance is used to quantify the probability distribution distance between it and a component ϕ_j^n in the online GMM ϕ^0 during the nth monitoring step, as shown in the following formula:

$$\mathrm{KL}\left(\Phi_i^0 \| \Phi_j^n\right)=\frac{1}{2}\left\{\begin{array}{l}\left(\boldsymbol{\mu}_j^n-\boldsymbol{\mu}_i^0\right)^{\mathrm{T}}\left(\boldsymbol{\Sigma}_j^n\right)^{-1}\left(\boldsymbol{\mu}_j^n-\boldsymbol{\mu}_i^0\right) \\ +\mathrm{tr}\left[\left(\boldsymbol{\Sigma}_j^n\right)^{-1}\left(\boldsymbol{\Sigma}_i^0\right)\right]-D-\ln\left(\dfrac{\det \boldsymbol{\Sigma}_j^n}{\det \boldsymbol{\Sigma}_i^0}\right)\end{array}\right\} \tag{13}$$

where μ_i^0 and $\sum_i^0$ are the mean and covariance matrix of ϕ_i^0. μ_j^n and $\sum_j^n$ are the mean vector and covariance matrix of ϕ_j^n. n is the monitoring time. *tr* is the trace of the matrix. *det* represents the determinant value of the matrix. D is the sample dimension.

The smaller the KL distance is, the smaller the difference between the two components. Therefore, the Gaussian component ϕ_j^n with the smallest difference between component ϕ_i^0 in online GMM ϕ^n and baseline GMM ϕ^0 can be found. The minimum matching KL distance of the final online GMM ϕ^n relative to the reference GMM ϕ^0 is:

$$KL_n\left(\Phi^0, \Phi^n\right)=\sum_{i=1}^{K} w_i^0 \min_{j=1}^{K}\left(\mathrm{KL}\left(\Phi_i^0 \| \Phi_j^n\right)+\ln\frac{w_i^0}{w_j^n}\right) \tag{14}$$

where ω_i^0 and ω_j^n are the weights of components ϕ_i^0 and ϕ_j^n, respectively.

The greater the difference between the online GMM and the baseline GMM is, the greater the probability migration index KL. Therefore, the damage state in the structure can be evaluated by the migration trend of the KL value.

4 Fatigue Crack Monitoring Experiment Under Time-varying Temperature

4.1 Fatigue tests and LW

The specimen is made of Al 6061 is shown in Figure 3(a). The plate used in the fatigue crack detection test has the mechanical properties provided in Table 1. An 8 mm hole was drilled at the center of the plate, and pre-cracks measuring 1 mm in size were introduced at both ends of the hole. Table 2 provides detailed parameters of PZT. The layout of the sensors used in the test is depicted in Figure 3(b).

Table 1: parameters of aluminum plate

Material	Density （kg/m3）	Young's modulus （Gpa）	Poisson's ratio
AL6061	2750	68.9	0.33

Table 2 parameters of PZT

PZT sensor model	diameter (mm)	thickness (mm)	Density (g/m3)
SM412	8	0.2	7.80

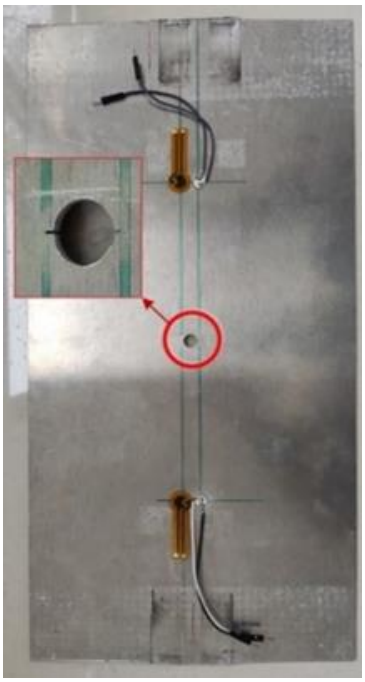

(a) Details of aluminum plate specimen

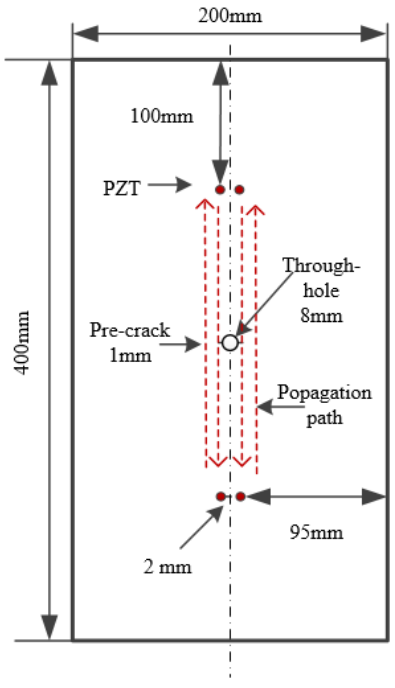

(b) Sensor layout diagram

Figure 3: Geometrical dimensions of aluminum plate and sensor.

A 2 mm thick plate was used as the test piece, and a Hanning-windowed sinusoidal tone burst with 4 cycles and 160 kHz was used as the excitation signal. Figure 4 illustrates the excitation signal used in this test.

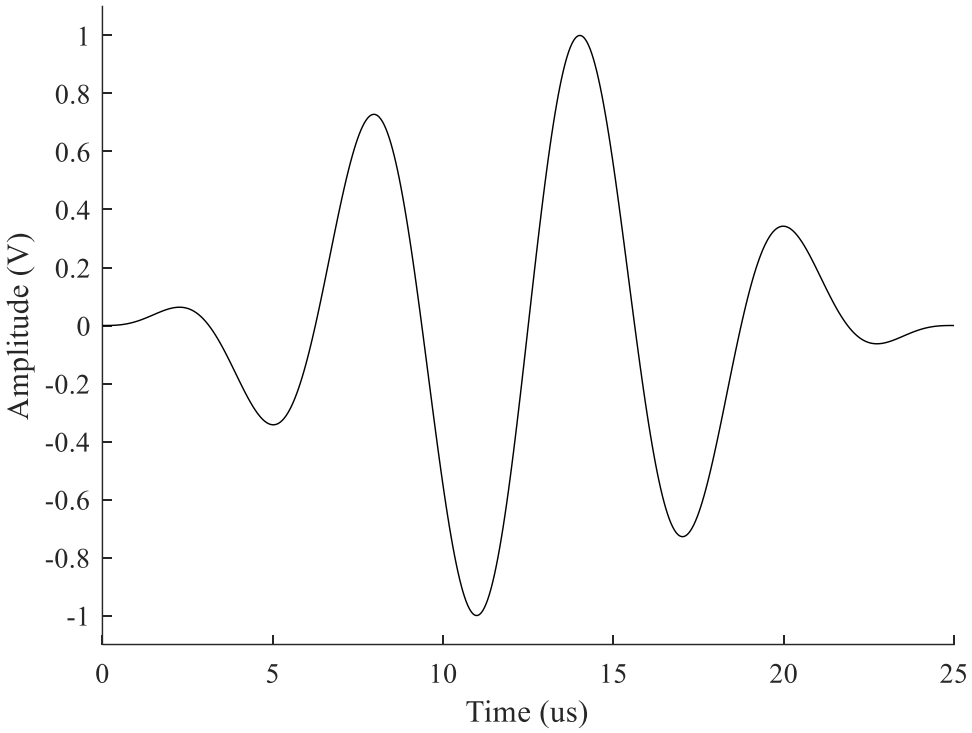

Figure 4: A signal of 4 cycles and 160 kHz central frequency. This signal is used as the excitation signal in this study.

The device is shown in Figure 5. Nine specimens (T1-T9) were used in this experiment, as shown in Figure 5(a). Different specimens were tested at different temperatures. T1 to T9 were tested at -40℃, -20℃, -10℃, 0℃, 25℃, 35℃, 55℃, 70℃ and 85℃ respectively. The system for detecting structural health in the presence of variable temperature fatigue cracks comprises four main components: SHM system, an light microscope , an environmental box, and a fatigue cycling system. The SHM system is responsible for collecting signals. A moving optical microscope monitors the size of the fatigue crack as it grows, as shown in Figure 5(b). The fatigue test is performed using an MTS Landmark hydraulic fatigue machine with a cycling frequency of 10 Hz, as depicted in Figure 5(c). The fatigue load is varied between 8Mpa and 80Mpa, and the loading frequency remains constant at 10 Hz. The loading spectrum for constant fatigue is presented in Figure 6.

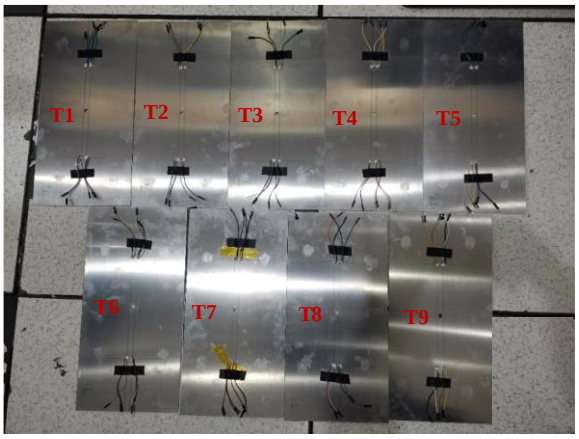

(a) nine specimens

(b)The traveling optical microscope

(c) MTS Landmark hydraulic fatigue machine and environment box

Figure 5: The overall experimental setup.

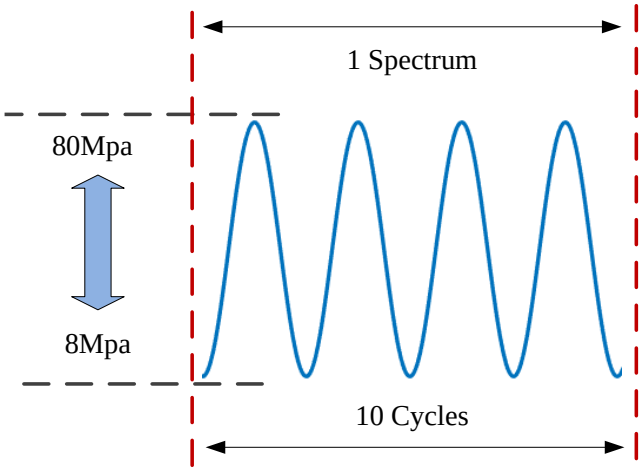

Figure 6: Constant Fatigue loading spectra for specimens.

Specimens T1–T9 are used for testing. Fatigue cracks are naturally generated during fatigue testing. Take the crack propagation length of 0.5mm as a measurement point

until the crack length is 5mm. Individual differences in PZT and control groups were considered, four groups of signals are measured under each crack length of each specimen, each PZT was used to excite and receive LW signals. After the fatigue testing, the collected data were sorted. The signals collected in the healthy state of specimens are named $m_1(t)$ $m_{36}(t)$ in the order of T1-T9. The signal collected when the crack is 0.5mm is named $m_{37}(t)$ $m_{54}(t)$ in the order of T1-T9. Similarly, the signals collected with crack lengths of $1mm$, $1.5mm$, $2mm$, $2.5mm$, $3mm$, $3.5mm$, $4mm$, $4.5mm$ *and* $5mm$ are named $m_{55}(t)$ $m_{216}(t)$ in the order of T1-T9. The above signals are used as training sets and the rest as test sets.

4.2 Extraction of information entropy

In the process of damage detection, it is necessary to continuously observe whether the Lamb signal changes to judge the damage state of the structure, which requires the extraction of damage indexes that can reflect the change in the Lamb wave signal. The Lamb wave signals of T2 specimen under different crack lengths is shown in Figure 7 (a). When the fatigue crack length is 1mm, the Lamb wave signals at different temperatures is shown in Figure 7(b). When the fatigue crack length is the same, the signals of different temperatures are very different. Therefore, time-varying temperature has a great influence on lamb signal.

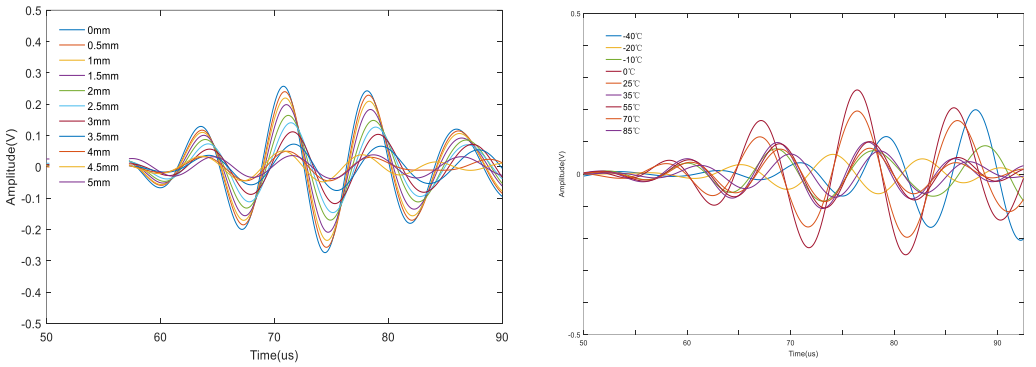

(a) Lamb wave signals at -20 ° C

(b) Lamb wave signals with crack length of 1mm

Figure 7: Lamb wave signal.

Traditional damage indexes such as phase shift and normalized amplitude need to select a fixed wave packet to extract the damage index. Due to the influence of time-varying temperature, different wave packets are superimposed on each other. The direct wave packets are difficult to extract accurately. Therefore, the extracted phase shift and normalized amplitude can not accurately represent the actual damage. The energy singular spectral entropy and power singular spectral entropy proposed in this paper do not need to select wave packets, and directly calculate the amount of information contained in PS the complete signal. Combined with energy change and

singular value spectrum analysis, the damage indexes ES and PS including time-varying temperature information and damage information are finally obtained, the results are shown in Figure 8(a)(b). To show the advantages of ES and PS, the traditional power information entropy and energy information entropy are also extracted, and the results are shown in the Figure 9(a)(b). According to the literature[30][31], the phase shift and normalized amplitude are also extracted, and the results are shown in Figure 10(a)(b).

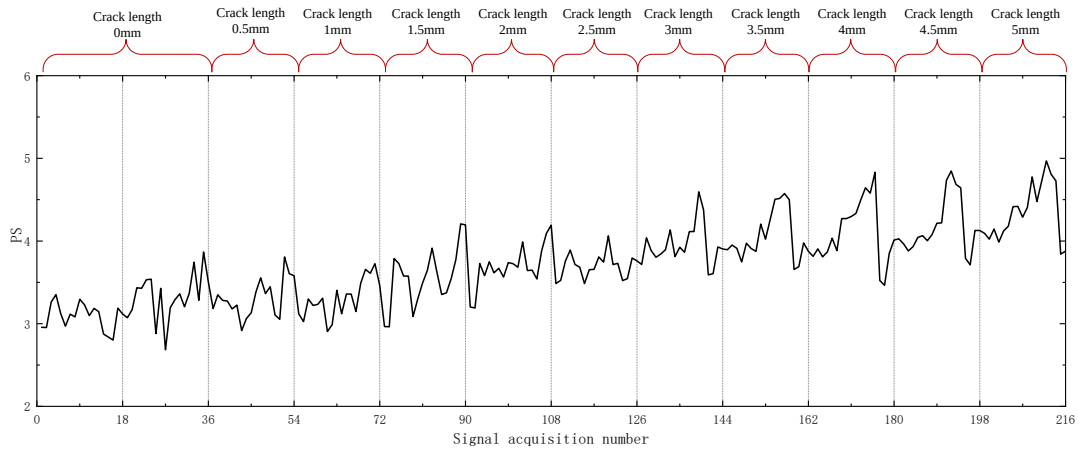

(a) PS

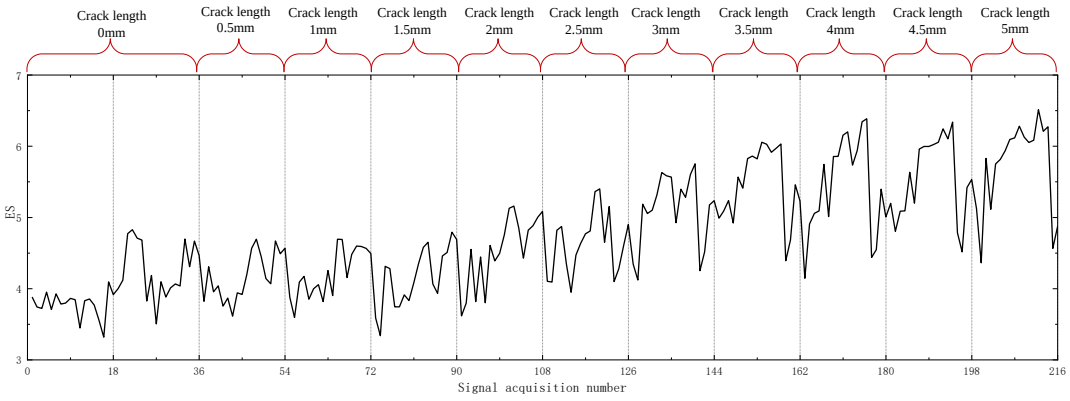

(b) ES

Figure 8: ES and PS information entropy trend.

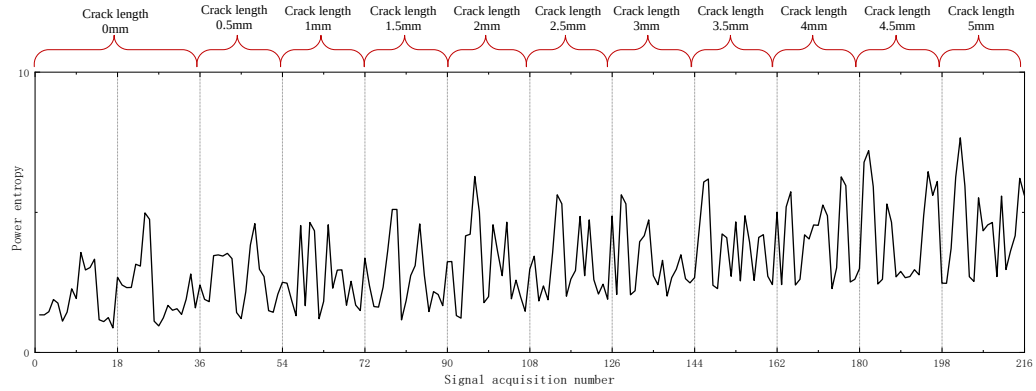

(a) Power information entropy

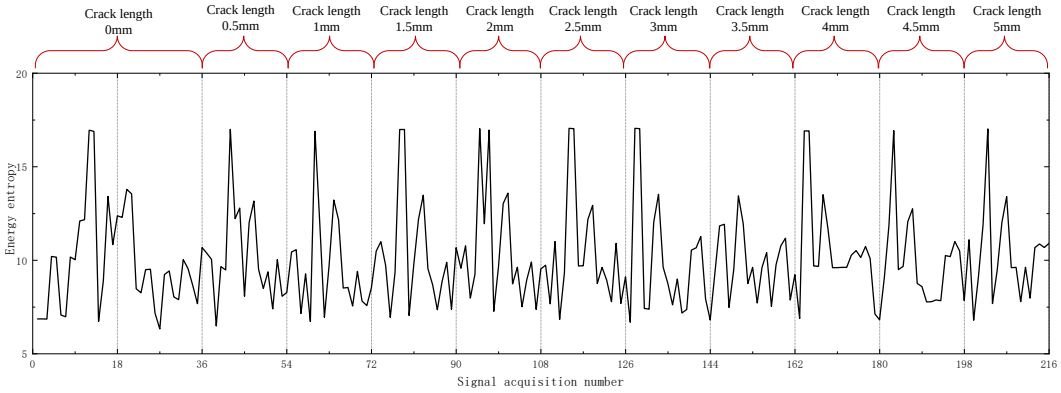

(c) Energy information entropy

Figure 9: Traditional information entropy trend.

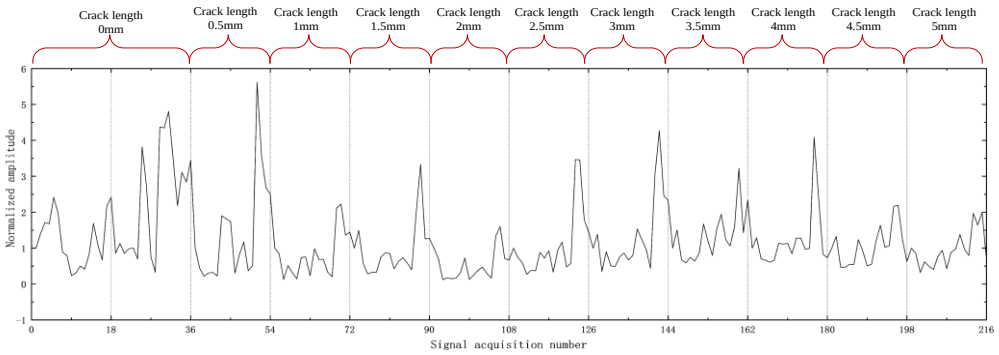

(a) normalized amplitude

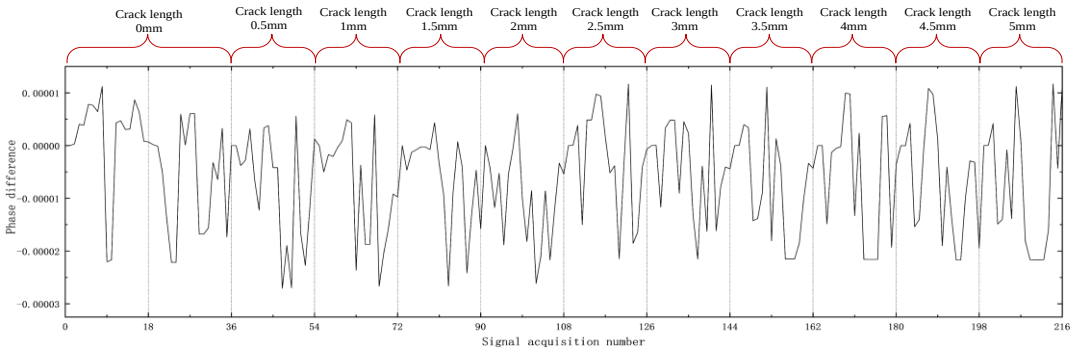

(b) Phase shift

Figure 10: Traditional damage indexes trend.

Under the condition of structural health, the damage indexes also changes when only the boundary conditions of the temperature change. It can be seen from Figure 8, 9 and 10 that there is no obvious linear relationship between information entropy or damage index and crack length under time-varying temperature environment. Therefore, it is difficult to quantitatively detect fatigue cracks by using traditional regression method. Comparing the information entropy with and without cracks shows that the crack cannot be judged only from the change in the value of this parameter, so the damage state cannot be evaluated by the conventional threshold setting method. Therefore, in the next section, GMM and migration index KL are established based on information entropy and traditional damage index, respectively. In this way, the damage status is evaluated and the pros and cons of the three types of damage indicators are compared.

4.3 Online Migration of the GMM

During online monitoring, the monitoring sample set needs to be updated continuously, and the update method is first-in first-out. If the number of monitoring times *n* is 1, the newly acquired online feature sample S_{19} is added to the end of S^0, and the first sample S_1 in S^0 is discarded, so the monitoring sample set is

$S^1 = \{S_2 | S_3, \cdots S_{19}\}$. The moving sample set is shown in Figure 9. In the experiment, the ES_r and PS_r corresponding to each signal constitute the damage indexes sample $S_K = [ES_K, PS_K]$, and the sample corresponding to the reference signal $m_1(t) \sim m_{18}(t)$ constitutes the reference feature sample set $S^0 = \{S_1 | S_2, \cdots S_{18}\}$. The moving sample set is shown in Figure 11.

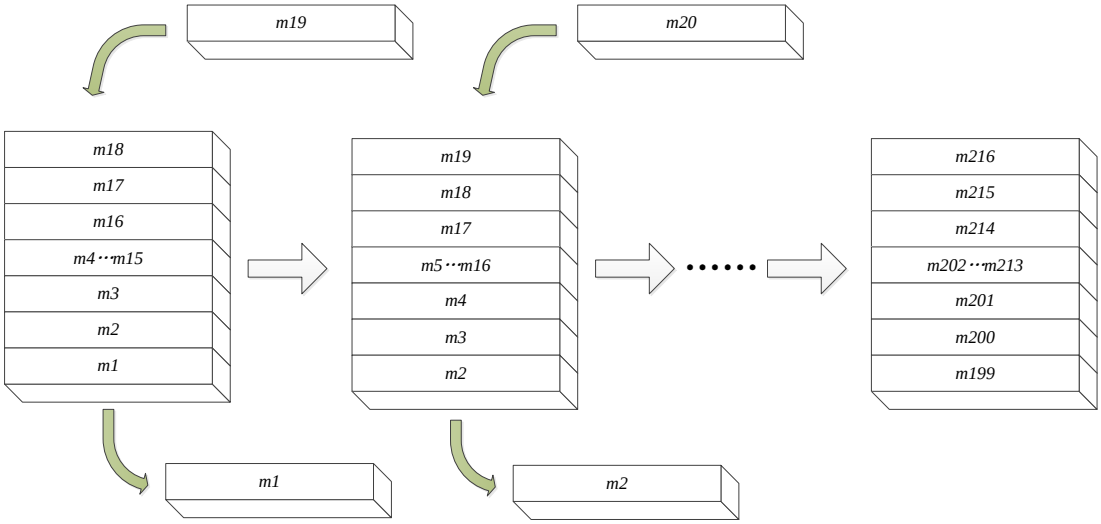

Figure 11: Schematic diagram of moving sample set.

In this study, the number of components *C* in the GMM is 3. The distribution of the GMM is characterized by a contour map, and each contour ellipse represents a Gaussian component. The online GMM base ES and PS during monitoring is shown in Figure 12. The online GMM base energy information entropy and power information entropy during monitoring is shown in Figure 13. The online GMM base traditional damage indexes (phase shift and normalized amplitude) during monitoring is shown in Figure 14. Figure 12(a) show when the structure has no cracks. Under the influence of the change in boundary conditions, some characteristic samples are randomly shifted However, the GMM probability distribution in Figure 12 (b) is basically consistent with the baseline GMM in Figure 12 (a), and the GMM distribution form does not change due to random changes in signal characteristics. After crack generation and propagation, the Gaussian component distribution in the GMM changes cumulatively, such as shrinkage and migration. Under the influence of cracks in the structure, the probability distribution of the online monitoring feature sample set changes cumulatively compared with the probability distribution of the baseline feature sample set, as shown in Figure 12(c)(d)(e)(f). As can be seen from Figure 13 and Figure 14, the GMM is not clear enough, and the cumulative change of Gaussian component distribution is small with the increase of fatigue crack length.

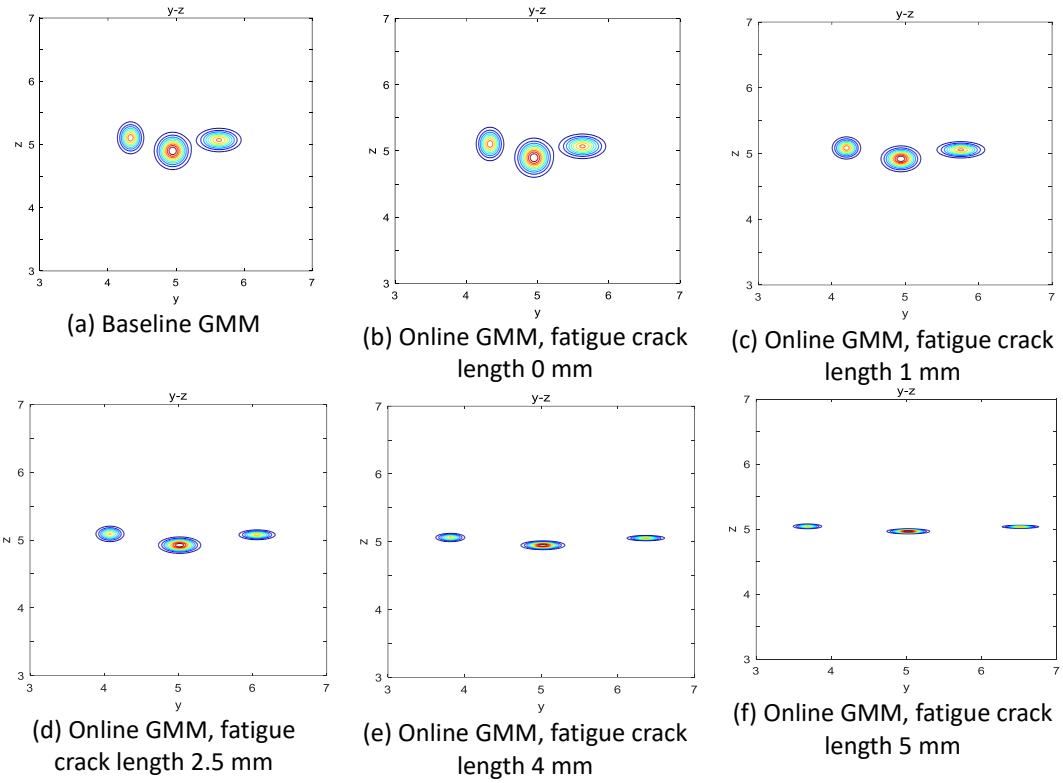

(a) Baseline GMM (b) Online GMM, fatigue crack length 0 mm (c) Online GMM, fatigue crack length 1 mm

(d) Online GMM, fatigue crack length 2.5 mm (e) Online GMM, fatigue crack length 4 mm (f) Online GMM, fatigue crack length 5 mm

Figure 12 GMM migration mechanism base on PS and ES.

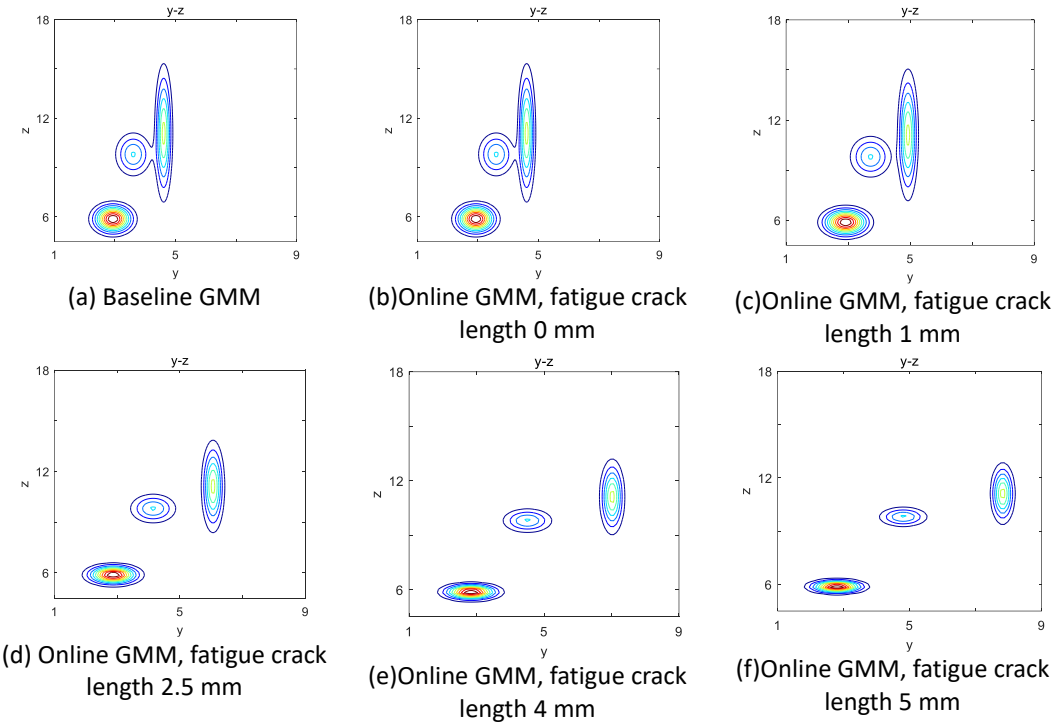

(a) Baseline GMM (b)Online GMM, fatigue crack length 0 mm (c)Online GMM, fatigue crack length 1 mm

(d) Online GMM, fatigue crack length 2.5 mm (e)Online GMM, fatigue crack length 4 mm (f)Online GMM, fatigue crack length 5 mm

Figure 13: GMM migration mechanism base on traditional information entropy.

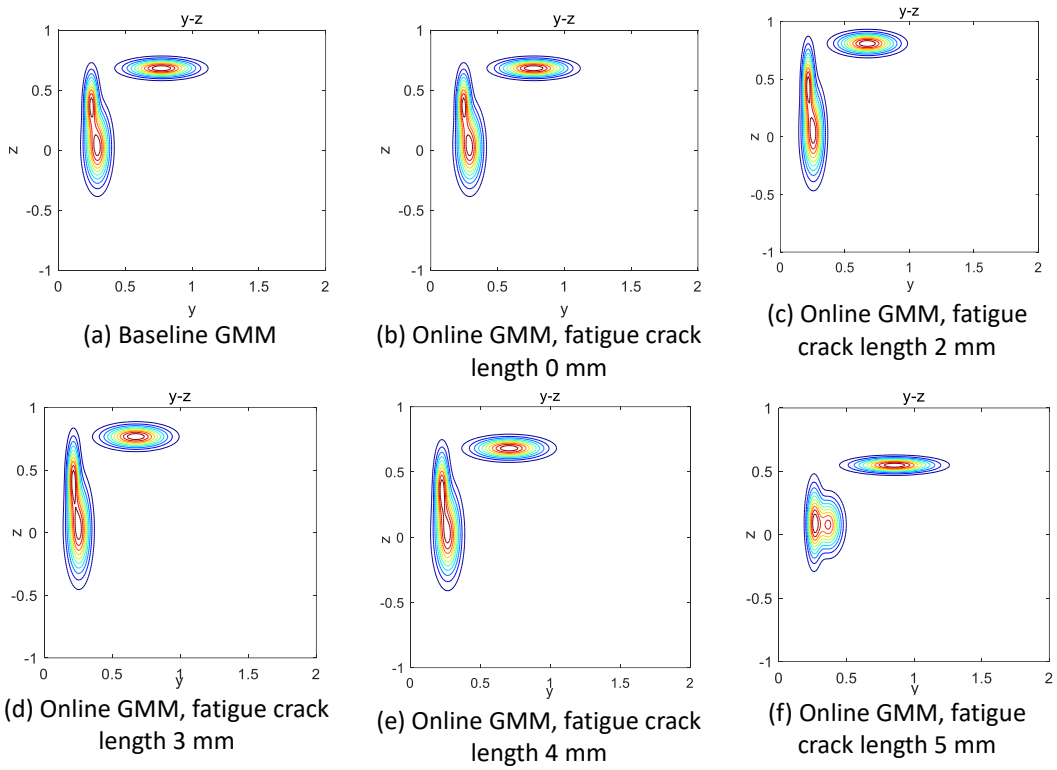

Fihure14: GMM migration mechanism base on traditional damage indexes.

4.4 Damage Monitoring Results and Analysis

The calculation results of GMM migration index KL shown in Figure 15. GMM migration index KL based on information entropy in the first 36 damage detection processes, the value of KL is basically 0, indicating that there is no simulated damage at this time. Although the temperature conditions are changing all the time in this stage, environmental factors have no impact on the probability migration index studied. From the 37th time, there is a difference between the online GMM and the baseline GMM, indicating that damage has occurred in the structure at this time. After that, the KL value shows an obvious ladder. The larger the KL value is, the larger the fatigue crack length on the structure. In the whole detection process, although the temperature conditions of the aluminum plate have been changing, the numerical change in KL accurately and reliably reflects the change in the fatigue crack on the structure. Although the KL trend based on the GMM using traditional damage index is consistent with the information entropy KL trend, the change with the crack growth is not obvious enough to be used as the threshold for detecting the crack length. According to the GMM migration index KL based on information entropy, the damage identification threshold can be easily set to realize the damage detection under time-varying temperature. Therefore, the GMM based on information entropy can facilitate reliable and stable damage detection in a time-varying environment. Compared with the detection results based on the information entropy damage factors

given in Figure 7, the detection reliability of fatigue crack propagation is significantly improved under the influence of time-varying temperature.

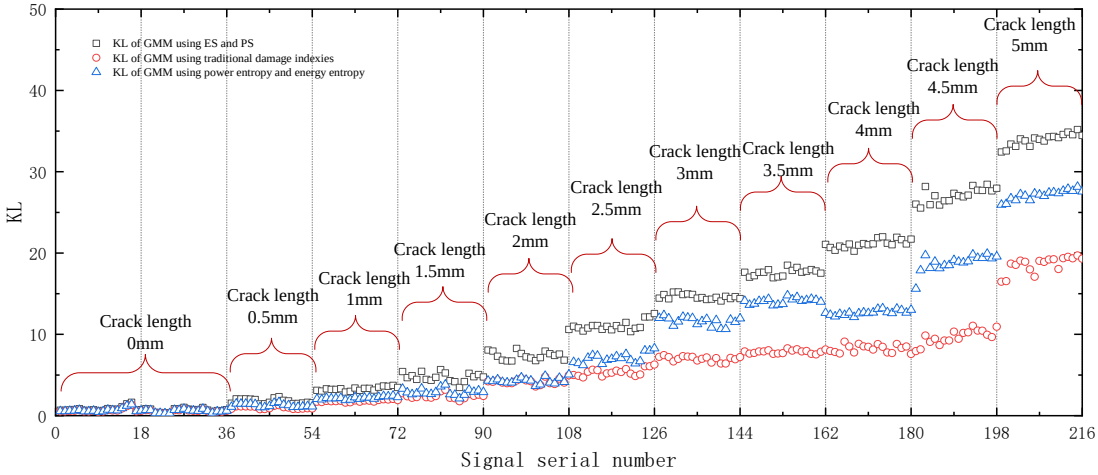

Figure 15: KL trend chart.

To further prove the reliability of this method, four groups of signals are randomly selected to construct the online migration index KL for verification. According to the method in Section 2.2, the PS and ES of the four groups of Lamb signals are extracted. The online migration index KL is established according to the methods in sections 3.2 and 3.3. The obtained test data is brought into the established online migration model for classification, and the classification matrix representing the classification accuracy is obtained as shown in Figure 16.

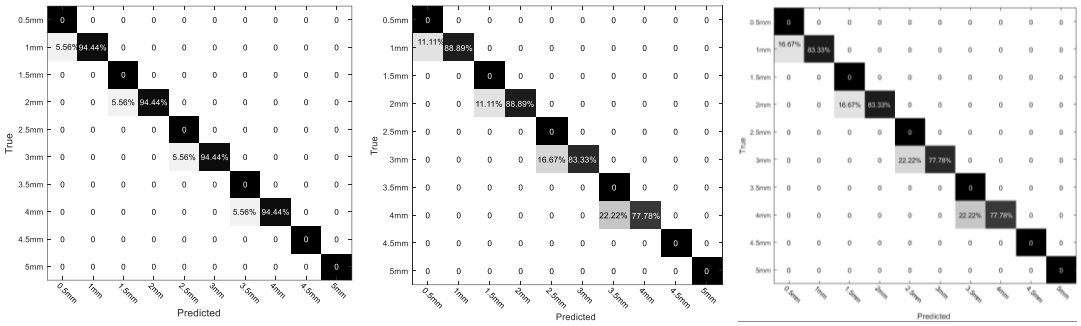

(a)Confusion matrix based on ES and PS

(b)Confusion matrix based on traditional information entropy

(c)Confusion matrix based on traditional damage indexes

Figure 16: Confusion matrix of test data.

In this test, signals with fatigue crack lengths of 1 mm, 2 mm, 3 mm and 4 mm under time-varying temperature are used as the test data set. Due to the weaker KL ladder type of the traditional damage index and traditional information entropy, it is difficult to determine the degree of damage from the test data. As shown in Figure 15 (a) confusion matrix based on information entropy, the classification accuracy of information entropy test data set is as high as 94.44%. As shown in Figure 15 (b) confusion matrix based on traditional information entropy, the classification accuracy

of the traditional damage index test data set is 83.33%. As shown in Figure 15 (c) confusion matrix based on traditional damage index, the classification accuracy of the traditional damage index test data set is 77.78%. Therefore, the on-line GMM base on ES and PS can effectively detect the fatigue crack length under time-varying temperature.

5. Conclusion

This paper proposed an online update damage detection method based on ES-PS-GMM under variable temperature environment. In this method, two new information entropy ES and PS are proposed. Then two information entropy are used to establish baseline GMM and online GMM. When the fault occurs and continues to spread, the KL shows a cumulative progressive trend. To validate the proposed method's effectiveness, fatigue crack experiments under variable temperature environments are conducted, and the results show its effectiveness for quantifying fatigue crack damage. The following conclusions are drawn:

The proposed GMM-based fatigue crack damage detection method using information entropy is effective for quantitatively detecting crack damage under time-varying temperature environments.

Two information entropy indexes (PS,ES) are extracted based on EEMD and SSA, which avoids the inaccurate problem of GMM established by traditional indexes under time-varying temperature. Compared with traditional information entropy (power entropy and energy entropy) and traditional damage index (normalized amplitude and correlation coefficient), the results show that ES and PS have higher robustness in time-varying temperature environment. It improves the stability of GMM method in detection structural damage of high-speed train under the environment of time-varying temperature.

References

[1] Rezaeianjouybari B, Yi S. Deep learning for prognostics and health management: State of the art, challenges, and opportunities[J]. Measurement, 2020, 163:107929.

[2] Zhou K, Zheng YB, Wu ZJ, et al. A reconstruction-based mode separation method of Lamb wave for damage detection in plate structures[J]. Smart Materials and Structures, 2019, 28(3):035033.

[3] Zhou DT, Huo LS, Song GB, et al. A feasibility study on monitoring of weld fatigue crack growth based on coda wave interferometry (CWI) [J]. Smart Materials and Structures, 2021, 30(9):095013.

[4] Liu X, Yu Y, Li J, et al. Leaky Lamb wave–based resin impregnation monitoring with noninvasive and integrated piezoelectric sensor network[J]. Measurement, 2022, 189: 110480.

[5] Wang B, Shi W, Zhao B, et al. A Modal Decomposition Imaging Algorithm for Ultrasonic Detection of Delamination Defects in Carbon Fiber Composite Plates

Using Air-Coupled Lamb Wave[J]. Measurement, 2022, DOI:10.2139/ssrn.4043684.
[6] Chen H, Zhang G , Fan D, et al. Nonlinear Lamb Wave Analysis for Microdefect Identification in Mechanical Structural Health Assessment[J]. Measurement, 2020, 164:108026.
[7] Shenfang Yuan, Jian Chen, Weibo Yang, et al. On-line crack prognosis in attachment lug using Lamb wave-deterministic resampling particle filter-based method[J]. Smart Materials and Structures, 2017(26): 085016.
[8] Junzhen Wang, Yanfeng Shen, Danyu Rao, et al. Physical-virtual time reversing of nonlinear Lamb waves for fatigue crack detection and quantification[J]. Mechanical Systems and Signal Processing, 2021, 107921.
[9] Shenbo Lu, Li Zhou. Fatigue crack monitoring of aerospace structure based on binary tree support vector machines[J]. PROC SPIE, 2017, 10170.
[10] Mao Y, Ma L, Ren Y, et al. Research on regional adjustment method of power grid operation and maintenance cost level based on information entropy considering multiple differences[J]. IOP Conference Series: Earth and Environmental Science, 2021, 680(1):012050.
[11] MA Hassan, MR Habib, RAA Seoud, et al. Wavelet-Based Multiresolution Bispectral Analysis for Detection and Classification of Helicopter Drive-Shaft Problems[J]. Journal of Dynamic Systems Measurement and Control, 2018, 140:061009.
[12] Shi Guoliang, Li Xiao, Jin Weidong, et al. Fault analysis of high-speed train running gear based on permutation and combination entropy [J]. Computer application research, 2014, 31(12): 3625-3627.
[13] Zhang Xuefeng, Ma Jing, Guan Wei, et al. Fault diagnosis of rolling bearing based on Gaussian mixture model[J]. Auto Time, 2018(12):188-190.
[14] Qiu L, Fang F, Yuan S F. Improved density peak clustering-based adaptive Gaussian mixture model for damage monitoring in aircraft structures under time varying conditions[J]. Mechanical Systems and Signal Processing, 2019, 126: 281-304.
[15] Banerjee S, Qing X L, Beard S, et al. Prediction of progressive damage state at the hot spots using statistical estimation[J]. Journal of Intelligent Material Systems And Structures. 2010, 21:595–605.
[16] Chakraborty D, Kovvali N, Papandreou-Suppappola A , et al. An adaptive learning damage estimation method for structural health monitoring[J]. Journal of Intelligent Material Systems & Structures, 2015, 26(2):125-143.
[17] Xie Fengyun, Jiang Yongqi, Feng Chunyu, et al. EEMD-KNN state recognition method for locomotive traction seat[J]. Machine Tool ＆ Hydraulics, 2022, 50(13):32-56.
[18] Zhang Liguo, Liu Wan, Zhang Shuqing, et al. Chaotic singular spectrum analysis and application based on improved phase space reconstruction algorithm[J]. Journal of Metrology, 2021, 42 (10):167-192.
[19] Barbosh M, Singh P, Sadhu, A. Empirical mode decomposition and its variants: a review with applications in structural health monitoring[J]. Smart Materials and Structures, 2020, 29(9):093001.

[20] Zhu YJ, Ni YQ, Jesus A, et al. Thermal strain extraction methodologies for bridge structural condition assessment[J]. Smart Materials and Structures, 2018, 27(10):105051.
[21] Yang Y, YuDejie, Cheng J. A roller bearing fault diagnosis method based on EMD energy entropy and ANN[J]. Journal of Sound and Vibration, 2006, 294(1):269-277.
[22] Altun E, Khan N M. Modelling with the Novel INAR(1)-PTE Process[J]. Methodology and Computing in Applied Probability, 2021:1-17.
[23] Qihang Yang. An Arrhythmia Diagnosis Method Based on the Combined Feature of Instantaneous Frequency and Power Spectrum Entropy[J]. Computer Science and Application, 2021, 11(3):495-504.
[24] Wang Q，Ma S X，Yue D.Identification of damage incomposite structures using Gaussian Mixture Model processed Lamb waves[J]. Smart Materials and Structures, 2018, 27(4):045007.
[25] Zhang Xuefeng, Ma Jing, Guan Wei, et al. Fault diagnosis of rolling bearing based on Gaussian mixture model[J]. Auto Time, 2018(12):188-190.
[26] Shi Yuanfeng, Zhu Zhengyan, Chen Peng, et al. Self reduced working modal analysis of state space model based on EM algorithm and modal form [J]. Engineering mechanics, 2021, 38 (09): 15-25.
[27] Dar-Shyang, Lee. Effective Gaussian Mixture Learning for Video Background Subtraction.[J]. IEEE Transactions on Pattern Analysis & Machine Intelligence, 2005, 27(08): 27-32.
[28] Yu J . Machine Tool Condition Monitoring Based on an Adaptive Gaussian Mixture Model[J]. Journal of Manufacturing Science & Engineering, 2012, 134(3):031004.
[29] Le J, Liao X ， Zhang L , et al. Distributionally robust chance constrained planning model for energy storage plants based on Kullback–Leibler divergence[J]. Energy Reports, 2021, 7(3):5203-5213.
[30] Phong B, DaoWieslaw J, Staszewski. Lamb wave based structural damage detection using cointegration and fractal signal processing[J]. Mechanical Systems and Signal Processing, 2014, 49:285-301.
[31] Jinsong Yang, Jingjing He, Xuefei Guan, et al. A probabilistic crack size quantification method using in-situ Lamb wave test and Bayesian updating[J]. Mechanical Systems and Signal Processing, 2016, 78.